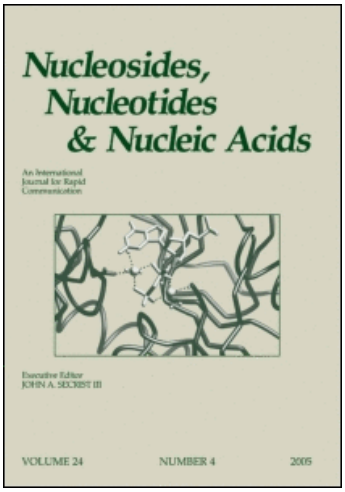

Nucleosides, Nucleotides and Nucleic Acids
Publication details, including instructions for authors and subscription information:
http://www.informaworld.com/smpp/title~content=t713597286

The Electron Affinities of Deprotonated Adenine, Guanine, Cytosine, Uracil, and Thymine

Edward C. M. Chen[a]; John R. Wiley[b]; Edward S. Chen[c]
[a] University of Houston Clear Lake, The Wentworth Foundation, Houston, Texas, USA [b] National Research Council of the National Academies, Washington, DC, USA [c] Baylor College of Medicine, Bioinformatics Research Center, Houston, Texas, USA

To cite this Article Chen, Edward C. M. , Wiley, John R. and Chen, Edward S.(2008) 'The Electron Affinities of Deprotonated Adenine, Guanine, Cytosine, Uracil, and Thymine', Nucleosides, Nucleotides and Nucleic Acids, 27: 5, 506 — 524
To link to this Article: DOI: 10.1080/15257770802088985
URL: http://dx.doi.org/10.1080/15257770802088985

Nucleosides, Nucleotides and Nucleic Acids, 27:506–524, 2008

ISSN: 1525-7770 print / 1532-2335 online
DOI: 10.1080/15257770802088985

Taylor & Francis
Taylor & Francis Group

THE ELECTRON AFFINITIES OF DEPROTONATED ADENINE, GUANINE, CYTOSINE, URACIL, AND THYMINE

Edward C. M. Chen,[1] John R. Wiley,[2] and Edward S. Chen[3]

[1]*University of Houston Clear Lake, The Wentworth Foundation, Houston, Texas, USA*
[2]*National Research Council of the National Academies, Washington, DC, USA*
[3]*Baylor College of Medicine, Bioinformatics Research Center, Houston, Texas, USA*

□ *Electron attachment rates and gas phase acidities for the canonical tautomers of the nucleobases and electron affinities for thymine, deprotonated thymine, and cytosine are reported The latter are from a new analysis of published photoelectron spectra. The values for deprotonated thymine are (all in eV) keto-N1-H, 3.327(5); enol-N3-H, 3.250(5), enol-C2OH, 3.120(5) enol-N1-H, 3.013(5), and enol-C4OH,3.123(5). The values for deprotonated cytosine, keto-N1-H, 3.184(5); trans-NH-H, 3.008(5); cis-NH-H, 3.039(5); and enol-N1-H, 2.750(5) and enol-O-H, 2.950(5). The gas phase acidities from these values are obtained from these values using experimental or theoretical calculations of bond dissociation energies. Kinetic and thermodynamic properties for thermal electron attachment to thymine are obtained from mass spectrometric data. We report an activation energy of 0.60 eV and electron affinity of thymine, 1.0(1) eV.*

Keywords Purines and pyrimidines; gas phase acidity; electron affinity; anion photoelectron spectra; negative ion mass spectrometry

1. INTRODUCTION

The electron affinities (E_a) and gas phase acidities (GPA) of adenine (A); guanine (G), cytosine (C), uracil (U), and thymine (T), collectively AGCUT or the purines, and pyrimidines (P) are important to electron transport and radiation damage in DNA. We obtained E_a from reduction potentials (ERED) and negative ion photoelectron spectra (NPS), and GPA from electron capture detector (ECD), negative chemical ionization mass spectrometry (NIMS), ion yield curves and non-aqueous acidities.[1–20] Since 1990, we reported adiabatic $E_a(AE_a)$ (in eV): G, 1.60(10); A, 1.09(5);

Received 10 September 2007; accepted 18 March 2008.
The authors were supported by the Wentworth Foundation.
Address correspondence to Edward C. M. Chen, University of Houston Clear Lake, The, Wentworth Foundation, 4039 Drummond, Houston, Texas, 77025, USA. E-mail: Edcmchen@gmail.com

C, 1.043(5); U, 0.99(2); T, 0.98(2); purine, 1.20(5); anthracene, 0.71(2) and acridine 1.08(2) with uncertainties in parentheses.[1–5,8–14] In 1998, we calculated E_a of Watson Crick AU, 1.27 eV; AT, 1.39 eV; and GC, 1.57 eV using semi-empirical multiconfiguration configuration interaction CURES-EC quantum mechanical calculations. These demonstrate the feasibility of electron conduction in DNA.[7] In 2001, we postulated excited state E_a for G and A to explain the formation of C(-) and T(-) in radiation damage.[9] We calculated the E_a of the deprotonated P ($E_a(P_{MinH})$) and first noted that A, G, U, and T are stronger gas phase acids than HCl since the $E_a(P_{MinH})$ are comparable to E_a(halogens).[5,10,19,20] Since 2000, others have measured GPA of A,C,U,T, alkyl-T and hypoxanthine using bracketing techniques.[21–29] We reviewed these in 2006 and reported acidities for the canonical tautomers of AGCUT from calculated $E_a(P_{MinH})$ and D(N-H,C-H). In 2007, Parsons et.al. assigned anion photoelectron spectra to the N1-H deprotonated isomers of the canonical tautomers and reported the first experimental $E_a(T_{MinN1H})$ and $E_a(C_{MinN1H})$.[30]

This article reports on (a) thermal electron attachment cross sections for AGCUT; (b) the electron affinity and activation energy for thermal electron attachment to thymine; (c) multiple E_a for C_{MinH} and T_{MinH}; (d) bond dissociation energies and GPA for C and T from quantum mechanical calculations; and (e) all the GPA of the canonical forms of AGCUT.

2. HISTORICAL BACKGROUND, METHODS OF EVALUATION, AND DEFINITIONS

Before 1960, the only E_a for organic molecules had been determined from reduction potentials (ERED) and the Nernst equation: $E_a(A) - E_a(B)$ = ERED(A)- ERED(B) as discussed by Streitweiser.[31] In 1963, Briegleb reviewed the calibration of these values to gas phase E_a.[32] In 1991, we measured the ERED of AGCUT, anthracene, acridine, nitrogen heterocyclics, and aromatic nitro compounds to obtain absolute E_a.[1–6,13,14,19,20] Lovelock observed thermal electron reactions in the ECD in 1961: AB + e(-) = AB(-) + E_a, or AB + e(-) = A + B(-) + E_1.[33] We obtained E_a and E_1 from responses at different temperatures using a kinetic model. This model is also applicable to thermal data from other techniques. In 2007, we reported multiple E_a and E_1 for SF_6 by combining data from ECD, NMS, magnetron, flowing afterglow, thermal charge transfer, alkali metal beam, electron beam, photon, and other swarm techniques over a temperatures of 50 K to 7500 K.[17] The thermal charge transfer studies give relative E_a or GPA which must be calibrated to absolute values. The onsets in electron or alkali metal beams give E_a from dissociation energies or ionization potentials. Photon methods give E_a from onsets. These methods have been reviewed.[19,20,34–38]

Both precision and accuracy are characteristics of the measurement procedure, not the value. Random errors are determined by repetition. Bias errors are only detected by measuring the same quantity with more than one method. When the procedures give the same value within the random error there are no systematic errors. The weighted average of $y_i(s_i)$ is the "best" value [$y(avg) = \Sigma\ (w_i\ y_i)\ /\ [\Sigma\ (w_i)]$; $s^2_{yavg} = 1/[\Sigma\ (w_i)]\ w_i = 1/s_i^{2}$]. Uncertainties should not be given to more than two figures. In 1999, we evaluated the E_a of over 200 organic molecules determined from reduction potentials.[4,5] We also have evaluated all the gas phase E_a of organic compounds listed in the National Institute of Standards and Technology (NIST) website.[13,14,19,20] The largest precise values were assigned to the AE_a and lower values to excited state E_a predicted from bonding (b) and antibonding (a) curves in dissociation channels.

The most common systematic error in the E_a is the assignment. This is particularly true when only one positive E_a is assumed. For O_2, the Hund Mulliken Rule predicts 54 total states from $O(^3P) + O(-)(^2P)$: 6 $O(-)(^2P)$ $\times$ 9 $O(^3P) = 54$ or 27 bonding spin orbital coupling states with positive E_a. The XY_2 Walsh diagrams predict two positive E_a for CS_2. These E_a have been measured in ECD and NPS experiments among others.[15,16, 38] The complexity of determining the electronic states for polyatomic molecules (anions) is described by Herzberg in the third volume in his trilogy.[39] "Every electronic state of a polyatomic molecule is characterized by a 3N-6 dimensional hypersurface. If the potential surface has no minimum, the electronic state is unstable; if the potential surface has at least one minimum, the electronic state is stable. [...] Potential surfaces with several minima occur not infrequently (sometimes corresponding to different isomers). Even in the simplest case, that of a triatomic molecule, the potential surface is three dimensional in a four dimensional space" (page 7; for non-linear molecules). The ultimate goal of our studies is to obtain such a surface for the reaction of electrons with the nucleobases.[1–20]

Two types of energy differences between an N electron system plus an electron and its N+1 anions are short range $E_a(SE_a)$ with the electrons in the valence shell and long range $E_a(LE_a)$ with repulsions balanced by dipole, quadrupole, or polarization attractions. The adiabatic E_a (AE_a) is always positive since it is an LE_a when all SE_a are negative: by convention E_a are positive for exothermic reactions The three anion energy differences are: E_a in the most stable forms; vertical $E_a(VE_a)$ in the neutral geometry, and vertical detachment energy(E_{vd}) in the anion geometry. The GPA or deprotonation energy (E_{dp}) is the energy for : $AH \rightarrow H(+) + A(-)$. In this article, the GPA is defined as $\Delta G(0K)$. Energies for specific deprotonation sites, X are: $E_{dpX} = IP(H) + E_{deaX}$: IP(H) is the ionization potential of hydrogen and the $E_{deaX} = D(R\text{-}H)—E_a(R)$. The $E_{dea} = -E_1$, the activation energy for dissociative electron attachment.

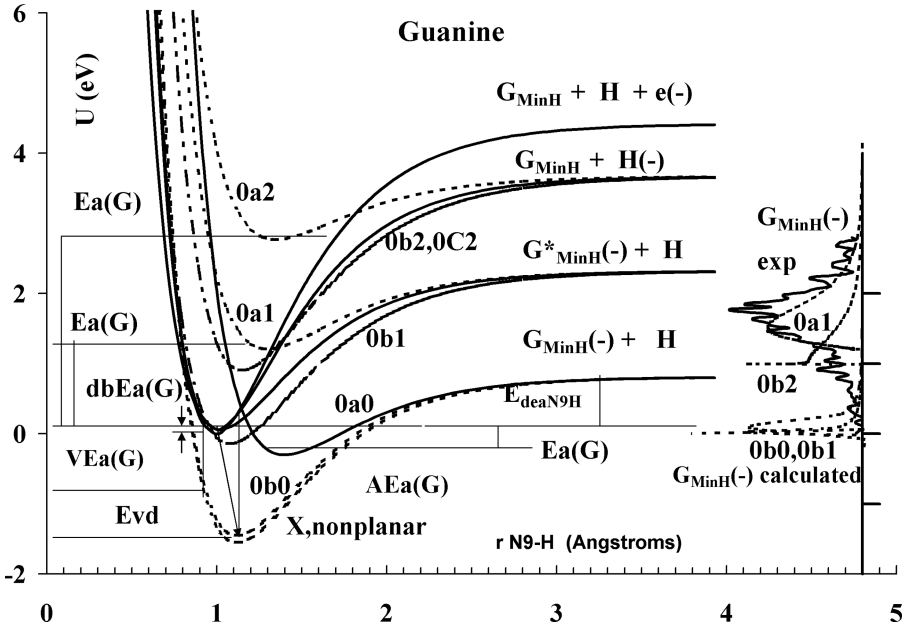

FIGURE 1 Ionic and neutral Morse potential energy curves for guanine to illustrate definitions. The experimental ion yield curve is taken from reference 42 while the calculated ion yield curves are obtained from the Morse potentials using the reflection method. The procedures for calculating curves are discussed above and in the literature.[8–17]

These definitions are illustrated by Herschbach Ionic Morse Person Empirical curves (HIMPEC) for guanine in Figure 1.[41] Guanine is chosen because it is presently the least characterized nucleobase. In the canonical tautomer of guanine, there are six single bonds: C-NH_2, N9-H, N-H, NH-H_a, NH-H_b and C8-H. There are three dissociation channels (m = 0–2): 0-[P_{MinX}(-) + H/NH_2]-n; 1-[P*$_{MinX}$(-) + H/NH_2]-n; 2-[H/NH_2(-) + P_{MinX}]-n in each dimension. The leading integer, m = 0, 1, 2 designates the channels and the second integer, n = 0–5 the single bonds. There are: 2-[(a&b) curves] × 3-[(0–2) channels] × 6-[(0–5) bonds] = 2 × 3 × 6 = 36 potentials in single bond channels in a given geometry. In addition, there are a multitude of long range X and C curves in reaction coordinates similar to Marcus parobalas. Three E_a (in eV) 1.60(10), 0.30(10) and 0.10(5) eV and ion yield curves were combined with -E_{dea} for the N9-H dimensions (see Table 1) and singlet triplet separations 1.2–2.4 eV from theoretical calculations to obtain the curves in Figure 1.[1,12,13,42]

3. THEORETICAL CALCULATIONS

The Configuration interaction or Unrestricted orbitals to Relate Experimental electron affinities to Self consistent values by estimating Electron Correlation (CURES-EC) procedure is a post self-consistent field

TABLE 1 Experimental and CURES-EC gas phase aciditie ΔG(298) electron affinities, bond dissociation energies, and energy for dissociative electron attachment in eV

	GPA (exp) (kcal/mole)	GPA(CEC) (kcal/mole)	GPA(CEC) (eV)	$E_a(P_{MinH})$ (eV)	D_0 (eV)	$-E_{dea}$ (eV)
Adenine						
N9-H	328(1)	329	14.3	3.40	4.10	0.70
NH-H	344(2)	342	14.9	3.06	4.25	1.19
NH-H	344(2)	343	14.9	3.06	4.27	1.21
C2-H	362(4)	365	15.9	2.35	4.55	–2.20˝
C8-H	366(4)	361	15.7	3.20	5.20	–2.00˝
Guanine						
N9-H	327(2)	327	14.2	3.50	4.10	0.60
NH-H	–328˝	328	14.3	3.33	4.19	0.86
NH-H	–333˝	332	14.5	3.26	4.18	0.92
N3-H	–329˝	329	14.3	3.43	4.04	0.61
C8-H	–356˝	356	15.5	3.30	5.10	–1.80˝
Cytosine						
N1-H	335(2)	337	14.6	[3.17]	4.00	0.83
NH-H	344(2)	344	14.8	[2.81]	4.14	1.33
NH-H	344(4)	340	14.8	[3.04]	4.16	1.12
C5-H	–379˝	379	16.5	2.15	4.95	–2.80˝
C6-H	–359˝	364	15.6	3.02	4.92	–1.90˝
Thymine						
N1-H	328(2)	328	14.3	[3.38]	4.10	0.72
N3-H	341(2)	342	14.9	3.66	4.87	1.21
CH2-H	370(2)	369	16.1	[1.50]	3.86	–2.36˝
C6-H	–365˝	364	15.6	3.22	5.08	–1.86˝
Uracil						
N1-H	328(2)	328	14.3	3.38	4.10	0.72
N3-H	341(2)	343	14.8	3.60	4.79	1.19
C5-H	379(4)	379	16.4	2.09	4.87	–2.78˝
C6-H	358(4)	358	15.6	3.22	5.09	–1.87˝

The data in [] indicate experimental values of the E_a of the deprotonated radicals. The data in –˝ are estimated values. The uncertainties in the experimental values of the GPA have been adjusted to reflect the agreement with the calculated values.

method to improve on semi-empirical calculations. The calculations were carried out with HYPERCHEM software on a desktop computer. The AE_a is the difference in the energy of the neutral and the anion at their global minimum. The calculations for AGCUT must be annealed to reach the global minimum geometries. The agreement with experiment is improved by adjusting multiconfiguration configuration interactions (MCCI). The maximum E_a is obtained without additional electron correlation in the neutral and four filled and three unfilled orbitals in the anion, RHF(4300) or the UHF procedure(UU00). The minimum E_a for a closed shell species is RHF(0043). The dissociation energies and electron affinities of the deprotonated purines and pyrimidines, $E_a(P_{MinH})$ also are calculated to match experiment.

3.1. Kinetic Model

The ECD and NMS studies are concentration jump experiments. A brief pulse of an ultra high purity sample is added to a quiescent background and the anion and/or electron concentrations measured as a function of temperature and amount injected. The reactions are:

$$AB + e(-) \underset{k_{-1}}{\overset{k_1}{\rightleftharpoons}} AB(-) \overset{k_2}{\rightarrow} A + B(-) \tag{1}$$

$$e(-) \text{ or } AB(-) + P(+) \text{ neutrals} \tag{2}$$

With $k_D = k_N =$ constant, at steady state:

$$K = \frac{k_1(k_N + k_2)}{(2(k_D(k_{-1} + k_N + k_2))} \tag{3}$$

The equilibrium constant for AB + e(-) = AB(-); [$K_{eq} = k_1/k_{-1}$] is related to an E_a by:

$$\text{Ln}K_{eq}T^{3/2} = \text{Ln}[Q_{an}] + \text{Ln}[S] + 12.43 + \frac{E_a}{RT} \tag{4}$$

The Q_{an} is ratio of the anion to neutral partition function and S is the ratio of the spin partition functions. $k_1 = A_1 T^{-1/2} \exp(-E_1/RT)$, $k_{-1} = A_{-1} T \exp(-E_{-1}/RT)$ and $k_2 = A_2 T \exp(-E_2/RT)$ The A_i and 12.43 are from fundamental constants, the translational partition function and the Debroglie wavelength of the electron.

$$K = \frac{[K_{eq}/2k_D]}{[1/(k_N + k_2) + (K_{eq}/k_1)]} \tag{5}$$

With fixed intercepts, one point in the limiting positive slope region gives the E_a/R, while one point in the negative slope region gives the E_1/R or $-E_{dea}/R$.

The slope of a standard Ln $KT^{3/2}$ versus 1000/T plot with one positive linear region is E_a/R and the intercept $12.43 + \text{Ln}((Q_{an}S_{an})(A_N/2A_D)$. For NIMS data, the second term is $\text{Ln}((Q_{an}S_{an})(A_N/A_D)$. At low temperatures, $k_{-1} << k_N$ and the pseudo linear plot gives a negative slope equal to E_1/R and an intercept Ln[(A_1/A_D)] The ECD curve for non-dissociative TEA is calculated from A_1, E_1, E_a, $Q_{an}S_{an}$, $A_D = A_N$ and Equation (5). With a given E_a and A_1 from the DeBroglie wavelength of the electron and the theoretical $Q_{an}S_{an}$ the only unknowns are A_D and E_1. When $k_2 >> (k_{-1} + k_N)$, the

intercept is Ln((A2/A-1)(A1/AD)) with a slope, (E1 + E2—E-1)/R. Thus, A2 and E2 also are required to calculate the ECD curve. The slope is also equal to -Edea/R. The Edea(AGCUT) have been measured in electron impact studies so that the only additional "unknown" is A2. A rigorous non-linear least squares data analysis including literature values and uncertainties was used to obtain multiple E1 and Ea.

Herschbach Ionic Morse Person Empirical Curves

The acronym, Herschbach Ionic Morse Person Empirical Curves (HIMPEC), gives credit to the early work by Herschbach and Person and emphasizes the empirical, not theoretical or experimental nature of the curves.[3,22–33]

The HIMPEC referenced to D_e (AB) = 0 are:

$$U(AB) = D_e(AB)\text{–}1 - 2\exp(-\beta(r - r_e)) + \exp(-2\beta(r - r_e))\tilde{} \quad (6)$$

$$U(AB)[-] = D_e(AB)\text{–}1 - 2k_A\exp(-k_B\beta(r - r_e)) + k_R\exp(-2k_B\beta(r - r_e)) - E_a(A, B)\tilde{} \quad (7)$$

$$D_e(AB[-] = [k_A^2/k_R]D_e(AB) \quad (8)$$

$$r_e(AB[-]) = [\ln(k_R/k_A)]/[k_B\beta(AB)] + r_e(AB) \quad (9)$$

$$\upsilon_e(AB[-]) = [k_Ak_B/k_R^{1/2}]\upsilon_e(AB) \quad (10)$$

$$VE_a = D_e(AB)(1 + 2k_A - k_R) - E_{dea} \quad (11)$$

r is the internuclear separation, r_e = r at the minimum of U(AB), $\beta = \nu_e(2\pi^2\mu/\ D_e[AB])^{1/2}$, μ, is the reduced mass. The E_{dea}, E_a, and VE_a are used to determine dimensionless constants k_A and k_R. Ion distributions, activation energies, anion frequencies or internuclear distances are used to obtain k_B which includes the additional mass of the electron.

3.3. Experimental Methods

A Hewlett Packard 5988 GC/MS system with He as a carrier gas and CO_2 or H_2 at 0.75 torr as the thermal electron source was used. The temperature of the ionization source was 476 to 543K. Equal moles were sequentially injected and mass spectra collected from m/z 30 to 300. The electron distribution was determined to be thermal based on the ratio of SF_5/SF_6. Stemmler and Hites have compiled mass spectra obtained with a similar instrument using methane as a dopant.[40] The other methods are described in the original articles. The photoelectron spectra and the derivative plots (dNPS) are obtained from the UNSCANIT program. The parabolic fits are from EXCEL.

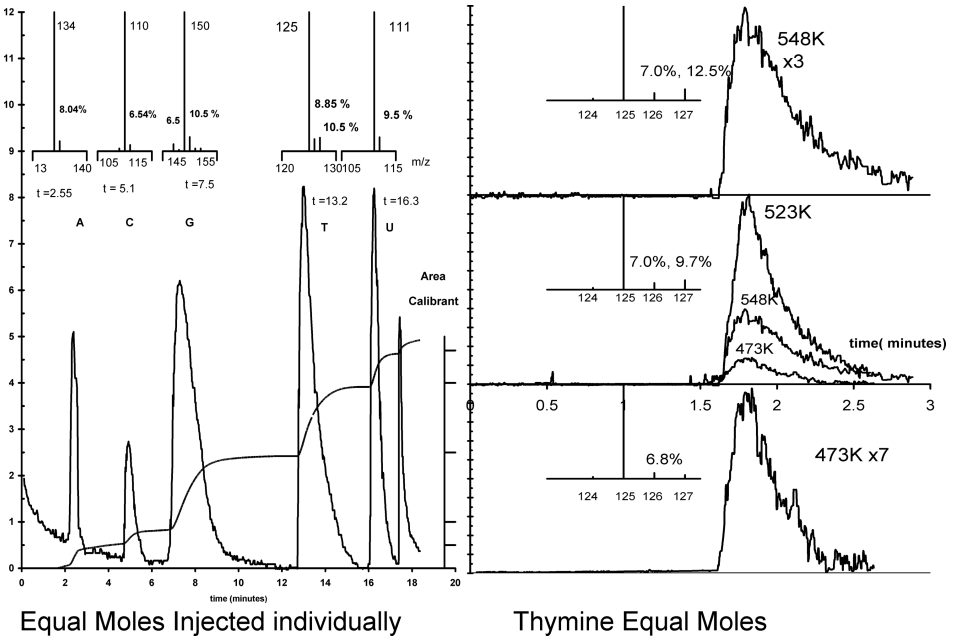

FIGURE 2 Chemical ionization negative ion mass spectra for the nucleobases collected by Wiley, Wentworth, Chen, and Chen in 1992. (See Refs.[8,13,43] for additional experimental details.)

4. RESULTS AND DISCUSSION

The primary results of this paper are the AE_a and E_1 of thymine from the NIMS data, the experimental and theoretical gas phase acidities of the nucleobases and the E_a of the deprotonated nucleobases. Parent negative ions are identified in unpublished NIMS in Figure 2. The molar responses are presented as $LnKT^{3/2}$ versus 1000/T in Figure 3 to obtain the AE_a and E_1 of thymine. Photoelectron spectra are provided in Figures 4 through 6 to illustrate an alternative method of determining electron affinities of not only the nucleobases but also the deprotonated nucleobases. In Table 1 are the "current best" experimental and calculated gas phase acidities for the canonical form of the nucleobases.

4.1. Negative Ion Mass Spectra

In 1975, Anbar and St. John observed the parent negative ion of thymine. In 1992, we measured the NIMS of AGCUT but did not publish them since they were considered to primarily be "bases." The formation of the deprotonated ions can now be explained from the GPA and electron affinities of the nucleobases and radical reactions such as $P^*(-) + H = P_{minH}(-) + H_2$. These are supported by the identification of the parent negative ion and hydrogen atom adducts in the mass spectra.

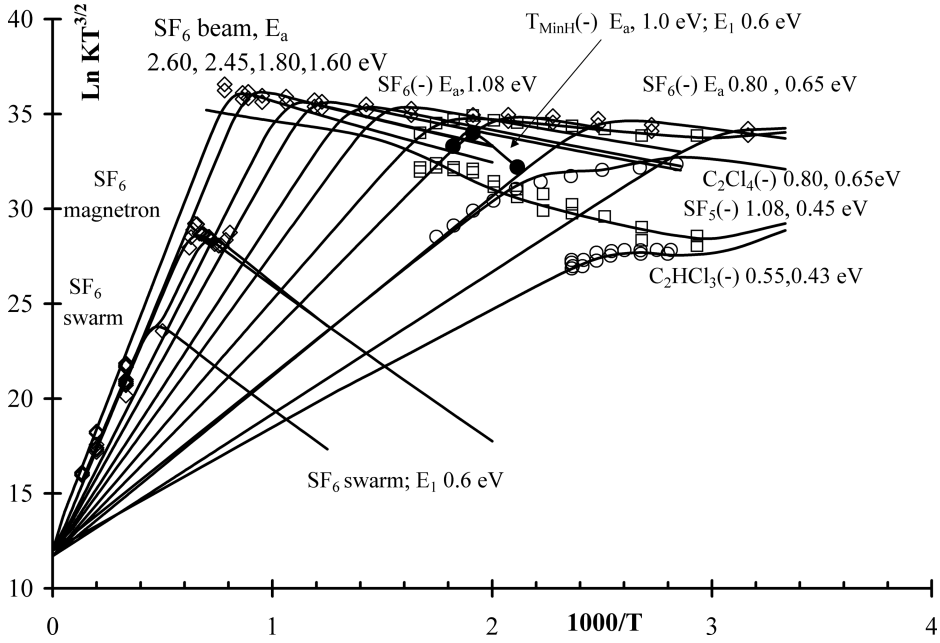

FIGURE 3 Negative ion mass spectra, electron beam, magnetron, and electron swarm data giving electron affinities, activation energies, and other kinetic and thermodynamic data for reactions of thermal electrons with SF_6, thymine, tetrachloroethylene, and trichloroethylene using the kinetic model for the electron capture detector. The positive slope for thymine gives an E_a of about 1 eV and the negative slope gives an E_1 of about 0.6 eV. The curves are calculated using Equation (5). (The data are discussed further in the Refs.[13,17])

The data obtained using H_2 as a dopant and cooling gas are shown as total ions versus time in Figure 2. We know of no other such data for the nucleobases collected in a single experiment. The reaction cross section for Thymine at 548 K was determined to be about the same as that of SF_6. This also was reported by Huels et.al. at a lower temperature [38]. The relative molar responses are: T = 1.5G = 2U = 3A = 3C for H_2 as a dopant and T = 2U = 3G = 3C = 4A for CO_2 as a dopant (not shown). In electron impact studies, the maximum cross section for the formation of T_{MinH} (-) at about 0.8 eV was an order of magnitude less than that of SF_6(-) at thermal energies. The relative cross sections for the deprotonated anions were reported as T = 2A = 3C = 3U = 40G. The much smaller response for guanine was noted.[39]

The experimental isotopic abundances for AGCUT shown in Figure 2 are larger than the theoretical values [1.08×(#C) + 0.37×(#N) + 0.016×(#H)] indicating the presence of parent negative ions. For thymine, the average of the four determinations of the [M]/[M-1] is 7.65% versus the calculated 6% giving about 1.7% of the parent negative ion. The large abundance of the M+1 ion indicates radical reactions. The precision of the experimental relative abundances for over fifty isotopic clusters containing

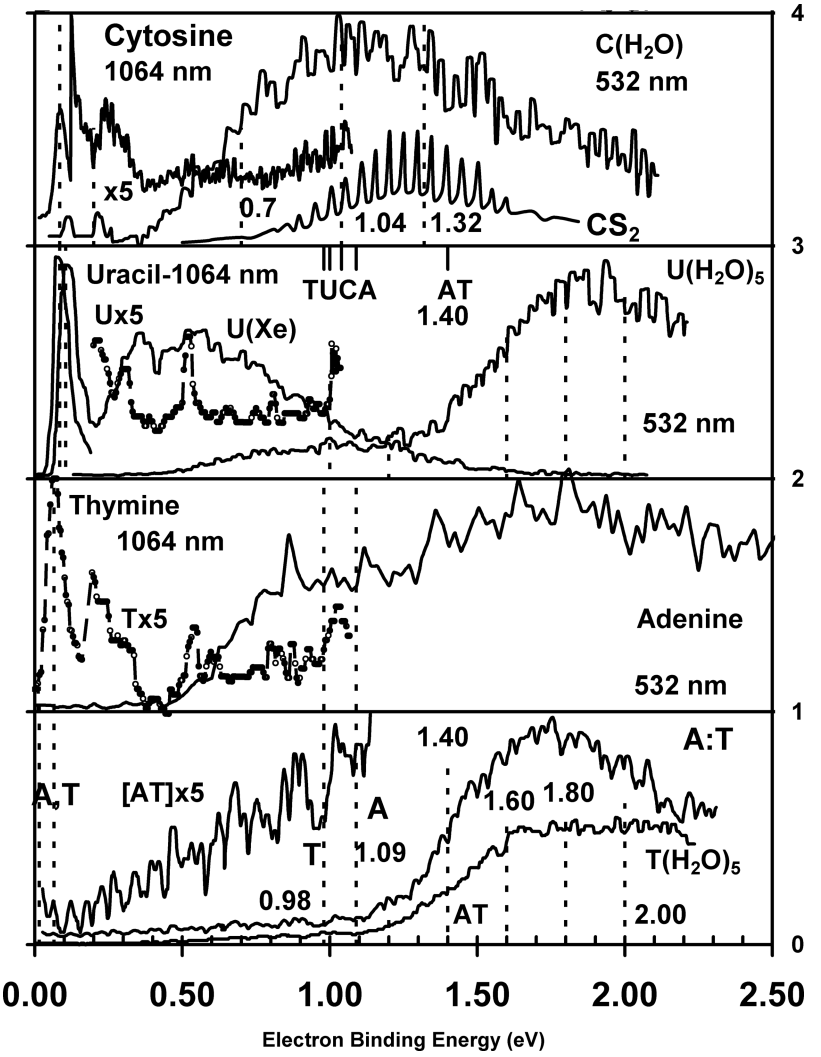

FIGURE 4 Negative ion photoelectron spectra taken from the literature[45–49] by electronically digitizing original figures.

C, H, O, and N was 0.3%. The temperature dependent data were obtained under the same conditions over about an hour.

The molar responses for $T_{MinH}(-)$, $SF_5(-)$, $SF_6(-)$, $C_2Cl_4(-)$ and $C_2HCl_3(-)$ and literature data for SF_6 are plotted in Figure 3 as $LnKT^{3/2}$ versus 1000/T. The data for SF_6 were used to obtain more than a dozen E_a and E_1 for SF_6. The ratio of the $SF_5(-)/SF_6(-)$ and the temperature dependence of $SF_6(-)$, $C_2Cl_4(-)$ and $C_2HCl_3(-)$ indicates that the electrons are thermalized. The E_a for C_2Cl_4 (0.80(2) eV and 0.65(2) eV) and C_2HCl_3 (0.55(2) eV and 0.43(2) eV) measured in ECD and/or reduction potentials studies were used to

calculate the curves in Figure 3. Also shown are calculated curves for $SF_6(-)$ and $SF_5(-)$. The three points for $T_{MinH}(-)$ and theoretical intercepts give an E_a about 1.0 eV for thymine in agreement with the ERED and NPS values and an activation energy, $-E_{dea}$, 0.6(2) eV in agreement with electron impact ion yield curves.[42]

4.2. Anion Photoelectron Spectra

In photoelectron spectroscopy, anions are formed in an ion source, mass selected and transferred to a second region where electrons are detached by a fixed energy laser. The negative ion photoelectron spectrum is a plot of electron intensity against the electron binding energy calculated from [EBE = hν- E_e]. Valence state anions with $E_a < 0.4$ eV are not observed since they undergo thermal detachment beyond the ion source. Dipole bound anions in the same geometry as the neutral with $E_a < 0.1$ eV are stable to autodetachment. In the analysis of NPS of small molecules, a single anion is assumed to be formed in the ion source and the onsets observed by photodetachment assigned to the E_a. The peak is assigned to the vertical detachment energy. In addition to simple transitions between the anion and the neutral, the onsets can be hot bands, transitions to excited states of the neutral or autodetachment from excited anion states.

The assignments for large molecules and complexes are complicated by rearrangement to other anions and/or photodissociation and formation of higher order complexes. These ions are then observed by absorption of a second photon. Random errors in NPS can be as low as 0.005 eV but systematic errors arise from assignments. These problems are illustrated by literature NPS for A,C,U,T and their complexes in Figure 4. Data for CS_2 obtained by Scheidt and Weinkauf using the same instrument are shown in Figure 4 (frame 3) to illustrate the attainable resolution. The low energy onset at about 0.6 eV for CS_2 is for the linear anion while the progression starting at about 0.9 eV is for transitions from the bent anion to the neutral.[43–46]

The peak widths for U and C are the same as for CS_2. The largest peaks in the spectra for isolated C, U, and T are for dipole bound anions as shown in Figures 4 (frame 1) to 4 (frame 3). Onsets for valence state anions are observed at higher energies. We assigned the highest energy onsets to the AE_a : (in eV) C, 1.04(2); U, 0.99; T, 0.98(2) based on the observation by Steenken and co-workers that the reduction potentials for C, U, and T are approximately equal as summarized in Figure 4 (frame 3).[1,18]

Valence state ions of U and C formed by complexation are shown in Figures 4 (frame 2) and 4 (frame 3). The hydration energy for cytosine is 1.32–1.04 = 0.28 eV. The onsets above 1.32 eV in the hydrated cytosine NPS are assigned to transitions to excited states of the neutral, detachment from excited anion states or higher order hydrates. The spectrum for AT

shown in Figure 4 was assigned to the Watson Crick form based on our predicted AE_a of 1.4 eV. The lower intensity onsets at the AE_a of A and T and the sequential onsets for pentahydrated anions of U and T are due to two photon processes. The hydration energy of about 0.2 eV per water for U and T suggests that Watson Crick AT(-) is the anion of thymine complexed to an excited state of adenine as postulated in 2001. The NPS of valence state adenine published in 2007 shown in Figure 4.1 was assigned to a rare tautomer with an AE_a less than 0.1 eV. In contrast, we assign the onset at 1.08 eV to the 0–0 band of the canonical tautomer based on literature E_a including that from the NPS of AT. Higher energy onsets are due to transitions to vibrational states of the neutral. Lower energy onsets are for other tautomers or excited states. Detachment from excited anion states observed in electron impact studies gives rise to the broad structure above 1 eV.

4.3. Anion Photoelectron Spectra of Deprotonated Cytosine and Thymine

In 2007, Parsons et al. assigned their NPS to the anions of T_{MinN1H} and C_{MinN1H} by following standard procedures. The experimental data and the "best" match for the Franck Condon simulated spectrum for the N1-H deprotonated anions are shown in Figure 5.[30] Additional structure is apparent. We explain this structure based on multiple anions and two photon processes as observed for the isolated bases. The E_a of the CH_2-H deprotonated isomer of T, 1.5 eV is the only such previously reported experimental value from NPS. We have reported AE_a of 3.40, 3.66 and 2.57

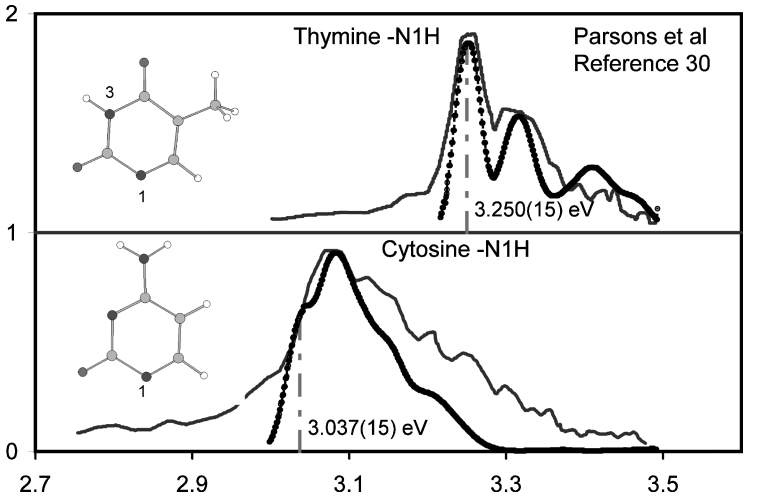

FIGURE 5 Anion photoelectron spectra simulated spectra and assignments for thymine and cytosine from Parsons et al.[30]

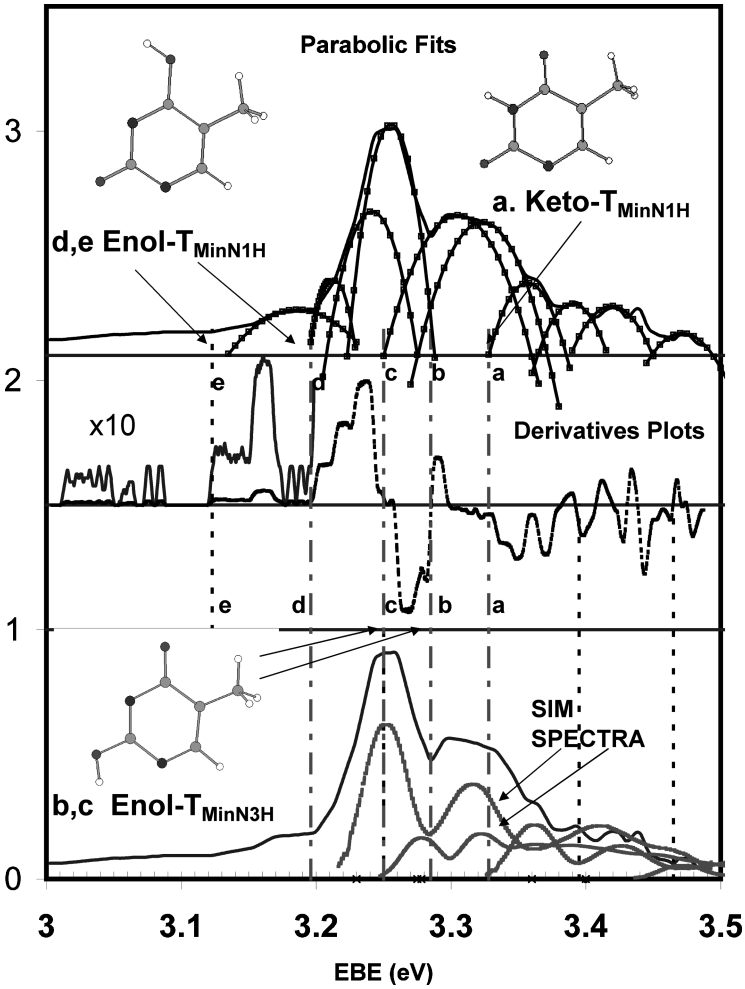

FIGURE 6 Photoelectron spectra; derivative of photoelectron spectra, and parabolic fits for thymine from Parsons et al.[30] and this work. The NPS and ion yield curves were electronically digitized from original figures in PDF and numerically differentiated using the UNSCANIT software.

eV for the N1-H, N3-H, and C6-H deprotonated isomers of the canonical tautomer of T. We now find that the AE_a of the deprotonated forms of the hydroxy tautomers are 3.0 and 3.5 eV which gives comparable GPA as observed in aqueous solutions.

In Figure 6 are the NPS, derivatives of the NPS, and parabolic fits used to obtain electron affinities. Also shown are the two simulated spectra shifted and scaled to fit the data. The onset at 3.327(2) eV is assigned to the N1-H tautomer and the vibrational transitions to the neutral. The onsets at 3.090(2) and 3.123(2) eV are assigned to the enol form of the N1-H deprotonated species based on the resolved triplet at 3.198(2), 3.211(2) and 3.227(2) eV. The onsets at about 3.250(15) are assigned to enol form of the

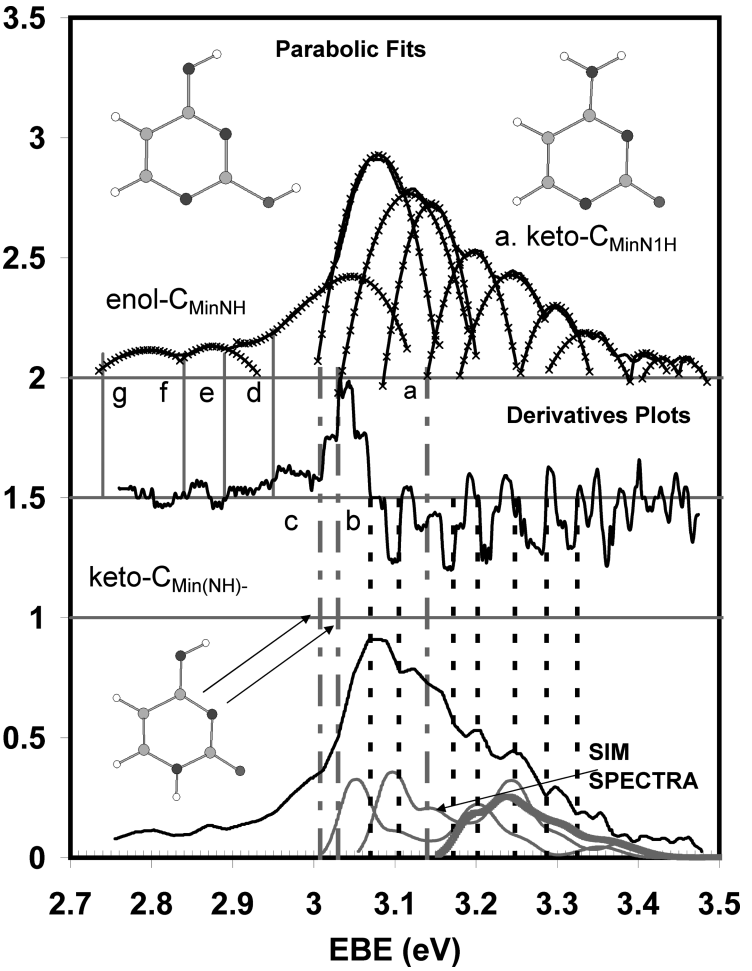

FIGURE 7 Photoelectron spectra; derivative of photoelectron spectra, and parabolic fits for cytosine from Parsons et al.[30] and this work. The NPS and ion yield curves were electronically digitized from original figures in PDF and numerically differentiated using the UNSCANIT software. The parabolic fits were obtained using least squares routines in EXCEL.

N3-H deprotonated anion. The absence of structure above 3.43 eV suggests a higher E_a for the N3-H deprotonated keto-tautomer.

The keto C_{MinN1H} and the $C_{MinNH\text{-}H}$ radicals have about the same calculated E_a, 3.0 eV. Parsons assigned the spectrum to the C_{MinN1H} (-) with an AE_a 3.037(15). In Figure 7 are the NPS, derivatives of the NPS, and parabolic fits to individual parts of the spectrum used to obtain electron affinities. Also shown are the three simulated spectra shifted to fit the data. We assign the onsets 3.037(2) and 3.012(2) to the NH-H deprotonated isomers. The onset at 3.139 eV is assigned to the AE_a of the N1-H deprotonated isomer.

The onsets below 3.0 eV are for the enol tautomers. All of these electron affinities are supported by CURES-EC calculations.

5. EXPERIMENTAL GAS PHASE ACIDITIES

The lowest GPA (most acidic hydrogens) for the canonical tautomers of A, C, U, and T are accurate and precise having been determined by more than one procedure. The GPA for G has only been obtained from NIMS data. These hydrogens are replaced by sugars in DNA. The secondary acidities are not well established. The D(N-H) for cytosine and thymine are used as prototypes in the CURES-EC procedure. The calculated GPA can be compared to site selective E_{deaNH} identified in electron impact spectra. The experimental C8-H acidity for hypoxanthine, 362 kcal/mole is used to estimate the C-8 acidities for adenine and guanine. This article presents updated GPA based upon the experimental E_a of the radicals, experimental data reported since 2003 and theoretical calculations.

The experimental and theoretical values of the N-H GPA for the most stable tautomers of AGCUT are summarized in Table 1. The most acidic hydrogens are the N1-H in CUT and the N9-H for A and G. The most acidic GPA of AGUT and the secondary N-H GPA for the keto tautomer of G are about the same and equal to that of HCl. The secondary N-H acidities for the other nucleobases are less acidic than HCl. The N3-H $\Delta G(0K)$ for U and T are significantly lower than the NH-H $\Delta G(0K)$ for C and A. The C-H GPA, are higher than the N-H GPA in agreement with experiment. The CURES-EC values are consistent with experiment. This is the only complete set of these quantities obtained by the same theoretical procedure.

6. CONCLUSIONS

The new results are:

1. The analysis of the chemical ionization mass spectrometry data to (a) report relative cross sections for the reaction of thermal electrons with the nucleobases; (b) identify residual parent negative ions of the nucleobases; (c) determine the rate constants and E_a for thymine; (d) determine the activation energy at 543K with an activation energy of about 0.6 eV; and (e) determine the AE_a of thymine, 1.0(1) eV.
2. The assignment of onsets in the NPS(T_{MinN1H}) to the adiabatic electron affinity of the keto-N1-H, 3.327(5); enol-N3-H, 3.250(5), enol-C2OH, 3.120(5) enol-N1-H, 3.013(5) and enol-C4OH,3.123(5).
3. The values for deprotonated cytosine, keto-N1-H, 3.184(5) eV; trans-NH-H, 3.008(5); cis-NH-H, 3.039(5); and enol-N1-H, 2.750(5) and enol-O-H, 2.950(5),

4. The calculation of a complete set of GPA, $E_a(P_{MinH})$, D(N-H) and D(C-H) for the canonical tautomers of AGCUT.

7. FUTURE WORK

In the recent analysis of the data for SF_6 which are partially shown in Figure 3, a protocol for obtaining potential energy surfaces for electron molecule reactions was presented. The first step is to compile all of the reported electron affinity values, including those from reduction potentials. Then the weighted averages are calculated. If all of these overlap, the best estimate of the AE_a is the weighted average. When there are significantly different averages then the largest value is the AE_a. The number of positive valence state E_a is predicted as discussed earlier for guanine. The significantly different values from all sources are assigned to predicted states. These and other data can be used to construct Herschbach Ionic Morse Person Empirical Curves. In the case of the nucleobases, tautomeric forms and geometries complicate the situation, giving additional local minima. Presently, few of the potential electon affinities in the NPS shown in Figure 4 have been obtained. Once this is done, there are many ion yield curves from electron impact studies which can be used to construct the HIMPEC. An example of this is the ion yield curve for G_{MinN9H} shown in Figure 1.

The only experimental electron affinity of guanine is from our reduction potentials in non-aqueous solvents. Thus the curves presented in Figure 1 are from the consolidation of a limited amount of experimental data. As such, they are as much prediction as they are an accurate representation. Their greatest value is in inspiring others to carry out additional experiments to test these predictions. As noted by Mulliken in 1972 in describing Morse potentials for I_2, "While the curves shown cannot possibly be quantitatively correct, they should be useful as forming a sort of zeroth approximation to the true curves."[50]

LIST OF ABBREVIATIONS

ECD	Electron Capture Detector
EI	Electron impact
NPS	Negative Ion Photoelectron Spectroscopy
CURES-EC	Semi-empirical procedure for predicting or verifying values
MCCI	Multiconfiguration configuration interaction
NIMS	Negative Chemical Ion Mass Spectrometry
AE_a	Adiabatic electron affinity
E_a	Electron affinity
$E_a(X,1,2)$	Specific state adiabatic electron affinity (X is the covalent ground state)
E_{dea}	Energy for dissociative electron attachment = $E_a(X)$- D_{XY}
E_1	Activation energy for thermal electron attachment = -E_{dea}

LE_a	Long Range electron affinity
SE_a	Short range electron affinity
VE_a	Vertical Electron Affinity
E_{vd}	Photodetachment or vertical detachment energy
NIST	National Institute of Science and Technology data base
Q_{an}	Partition function ratio of anion to neutral without spin factors
S_{an}	Spin partition function ratio
q_e	Translational partition function of the electron
g_i	Multiplicities for anion, neutral and electron.
K	Molar response or response calculated from rate constants.
K_{eq}	Equilibrium constant for electron molecule reactions
k_1	Rate constant for thermal electron attachment = $A_1 T^{-1/2} \exp(E_1/RT)$
k_{-1}	Rate constant for thermal electron attachment = A_{-1}Texp(E-$_1$/RT)\
k_2	Rate constant for thermal electron attachment = A_2Texp(E_2/RT)\
k_N, k_D	Pseudo unimolecular recombination coefficient for electrons and ions

REFERENCES

1. Wiley, J.R.; Robinson, J.M.; Ehdaie, S.; Chen, E.C.M.; Chen, E.S.; Wentworth, W.E. The determination of absolute electron affinities of the purines and pyrimidines in DNA and RNA from reversible reduction potentials. *Biochem. Biophys. Res. Commun.* **1991**, 180, 841–845.
2. Chen, E.C.M.; Wentworth, W.E. A comparison of experimental determinations of electron affinities of pi charge transfer complex acceptors. *J. Chem. Phys.* **1975**, 63, 3183–3189.
3. Chen, E.C.M.; Wentworth, W.E. Experimental determination of electron affinities of organic molecules. *Mol. Cryst. Liq. Cryst* **1989**, 171, 271–285.
4. Chen, E.S.; Chen, E.C.M.; Sane, N.; Talley, L.; Kozanecki, N.; Schulze, S. Classification of organic molecules to obtain electron affinities from half wave reduction potentials: The aromatic hydrocarbons. *J. Chem. Phys.* **1999**, 110, 9319–9329.
5. Chen, E.S.; Chen, E.C.M.; Sane, N.; Schulze, S. Classification of organic molecules to obtain electron affinities from half-wave reduction potentials: Cytosine, uracil, thymine, guanine and adenine. *Bioelectrochemistry and Bioenergetics* **1999**, 48, 69–78.
6. Chen, E.S.; Chen, E.C.M.; Sane, N. The electron affinities of the radicals formed by the loss of an aromatic hydrogen atom from adenine, guanine, cytosine, uracil, and thymine. *Biochem. Biophys. Res. Commun.* **1998**, 246, 228–230.
7. Chen, E.S.; Chen, E.C.M. A proposed model for electron conduction in DNA based upon pairwise anion π stacking: electron affinities and ionization potentials of the hydrogen bonded base pairs. *Bioelectrochemistry and Bioenergetics* **1998**, 46, 15–19.
8. Chen, E.C.M.; Chen, E.S. Negative ion mass spectra, electron affinities, gas phase acidities, bond dissociation energies, and negative ion states of cytosine and thymine. *J. Phys. Chem. B* **2000**, 104, 7835–7844.
9. Chen, E.S.; Chen, E.C.M. The negative ion states of molecules: adenine and guanine. *Biochem. Biophys. Res. Commun.* **2001**, 289, 421–426.
10. Chen, E.C.M.; Herder, C.; Chen, E.S. The experimental and theoretical gas phase acidities of adenine, guanine, cytosine, uracil, thymine and halouracils. *J. Mol. Structure.* **2006**, 79, 126–133.
11. Chen, E.C.M.; Chen, E.S. Thermal electrons and watson crick AT(−). *Chem. Phys. Letters* **2007**, 435, 331–335.
12. Chen, E.C.M.; Herder, C.; Chen, E.S. The ground and excited state electron affinities of cytosine and trans-azobenzene. *Chem. Phys. Letters* **2007**, 440, 180–186.
13. Chen, E.S.; Chen, E.C.M. *The Electron Capture Detector and the Study of Reactions with Thermal Electrons.* Wiley, New York, 2004.
14. Chen, E.C.M.; Chen, E.S. Molecular electron affinities and the calculation of the temperature dependence of the electron-capture detector response. *J. Chromatography A* **2004**, 1037, 83–106.

15. Chen, E.C.M.; George, R.; Carr, S.; Wentworth, W.E.; Chen, E.S. Determination of multiple electron affinities of carbon disulfide using electron-capture detection. *J. Chromatography A* **1998**, 811, 250–255.
16. Chen, E.C.M.; Herder, C.; Chang, W.; Ting, R.; Chen, E.S. Experimental determination of spin–orbital coupling states of O_2(-). *J. Phys. B.* **2006**, 3, 2317–2333.
17. Chen, E.C.M.; Chen, E.S. Electron affinities and activation energies for reactions with thermal electrons: SF_6 and SF_5. *Physical Rev. A* **2007**, 76, 032508–1.
18. Steenken, S.; Telo, J.P.; Novais, H.M.; Candeias, L.A. One-electron-reduction potentials of pyrimidine bases, nucleosides and nucleotides in aqueous solution. consequences for DNA redox chemistry. *J. Am. Chem. Soc.* **1992**, 114, 4701–4709.
19. National Institute of Standards and Technology (NIST) Chemistry WebBook, 2005, Available online at http://webbook.nist.gov/; accessed September 1, 2007.
20. Christodoulides, A.A.; McCorkle, D.L.; Christophorou, L.G. *Electron Affinities of Atoms, Molecules and Radicals.* Academic Press, New York, 1984.
21. Rodgers, M.T.; Campbell, S.; Marzluff, E.M.; Beauchamp, J.L. Low-energy collision-induced dissociation of deprotonated dinucleotides: Determination of the energetically-favored dissociation pathways and the relative acidities of the nucleic acid bases. *Int. J. Mass Spectr. Ion Processes* **1994**, 137, 121–149.
22. Freitas, M.A.; Shi, S.D.-H.; Hendrickson, C.L.; Marshall, A.G. Gas-phase RNA and DNA ions. 1. H/D Exchange of the $[M—H]^-$ anions of nucleoside 5′-monophosphates (GMP, dGMP, AMP, dAMP, CMP, dCMP, UMP, dTMP), ribose 5-monophosphate, and 2-deoxyribose 5-monophosphate with D_2O and D_2S. *J. Am. Chem. Soc.* **1998**, 120, 10187–10193.
23. Feng, W.Y.; Austin, T.J.; Chew, F.; Gronert, S.; Wu, W. The mechanism of orotidine 5′-monophosphate decarboxylase: catalysis by destabilization of the substrate. *Biochemistry* **2000**, 39, 1778–1783.
24. Kurinovich, M.A.; Lee, J.K. The acidity of uracil from the gas phase to solution: The coalescence of the N1 and N3 sites and implications for biological glycosylation. *J. Am. Chem. Soc.* **2000**, 122, 6258–6262.
25. Sharma, S.; Lee, J.K. Acidity of adenine and adenine derivatives and biological implications. A computational and experimental gas-phase study. *J. Org.Chem.* **2002**, 67, 8360–8365.
26. Kurinovich, M.A.; Lee, J.K. The acidity of uracil from the gas phase to solution: The coalescence of the N1 and N3 sites and implications for biological glycosylation. *J. Am. Soc. Mass Spectrometry* **2002**, Pages 985–995.
27. Fu, Y.; Sharma, S.; Lee, K. Annual Meeting American Society of Mass Spectrometry, 2004, Abstract 278.
28. Sun, X.; Lee, J.K. Acidity and proton affinity of hypoxanthine in the gas phase versus in solution: Intrinsic reactivity and biological implications. *J. Org. Chem.* **2007**, 72, 6548–6555.
29. Miller, T.M.; Arnold, S.T.; Viggiano, A.A.; Miller, A.E.S. Acidity of a nucleotide base: Uracil. *J. Phys. Chem. A* **2004**, 108, 3439–3446.
30. Parsons, B.F.; Sheehan, S.M.; Yen, T.A.; Neumark, D.M.; Wehres, N.; Weinkauf, R. Anion photoelectron imaging of deprotonated thymine and cytosine. *Physical Chemistry Chemical Physics* **2007**, 9, 3291–3297.
31. Streitweiser, A.S. *Molecular Orbital Theory for Organic Chemists.* Wiley, New York, 1961.
32. Brieglieb, G. Electron affinity of organic molecules. *Angewante Chemie International Edition* **1964**, 3, 1027–1031.
33. Lovelock, J.E. Affinity of organic compounds for free electrons with thermal energy: Its possible significance in biology. *Nature* **1961**, 189, 729–732.
34. Page, F.M.; Goode, G.C. 1969, *Negative Ions and the Magnetron.* Wiley-Interscience, New York
35. Dillard, J.G. Negative ion mass spectrometry. *Chem. Rev.* **1973**, 73, 589–643.
36. Kebarle, P.; Chowdhury, S. Electron affinities and electron-transfer reactions. *Chem. Rev.* **1987**, 87, 513–534.
37. Kleyn, A.W.; Moutinho, A.M.C. Negative ion formation in alkali-atom-molecule collisions. *J. Phys. B* **2001**, 34, R1–R44.
38. Rienstra-Kiracofe, J.C.; Tschumper, G.S.; Schaefer, H.F.; Nandi, S.; Ellison, G.B. Atomic and molecular electron affinities: photoelectron experiments and theoretical computations. *Chem. Rev.* **2002**, 102, 231–282.

39. Schiedt, J.; Weinkauf, R. Photodetachment photoelectron spectroscopy of mass selected anions: anthracene and the anthracene-H 2 O cluster. *Chem. Phys. Lett.* **1997**, 266, 201–205.
40. Herzberg, G. *Molecular Spectra and Molecular Structure*. D. Van Nostrand Company, Princeton, NJ, 1967.
41. Herschbach, D.R. Molecular dynamics of elementary chemical reactions (Nobel Lecture). *Angewandte Chemie International Edition* **1987**, 26, 1221–1243. This acronym was accepted by Prof. Herschbach, after noting he was simply following W.B. Person.
42. Abdoul-Carime, H.; Gohlke, S.A.; Illenberger, E. Site-specific dissociation of DNA bases by slow electrons at early stages of irradiation. *Phys. Rev. Lett.* **2004**, 92, 168103.
43. Stemmler E.A.; Hites R.A. *Electron Capture Negative Ion Mass Spectra of Environmental Contaminants and Related Compounds*. VCH, New York, 1988.
44. Anbar, M.; St. John, G.A. Formation of negative ions under inverted field ionization conditions. *Science* **1975**, 190, 781–782.
45. Huels, M.A.; Hahndorf, I.; Illenberger, E.; Sanche, L. Resonant dissociation of DNA bases by subionization electrons. *J. Chem. Phys.* **1998**, 108, 1309–1312.
46. Hendricks, J.H.; Lyapustina, S.A.; de Clercq, H.L.; Snodgrass, J.T.; Bowen, K.H. Dipole bound, nucleic acid base anions studied via negative ion photoelectron spectroscopy. *J. Chem. Phys.* **1996**, 104, 7788–7791.
47. Schiedt, J.; Weinkauf, R.; Neumark, D.M.; Schlag, E.W. Anion spectroscopy of uracil, thymine and the amino-oxo and amino-hydroxy tautomers of cytosine and their water clusters. *Chem. Phys.* **1998**, 239, 511–524.
48. Radisic, D.; Bowen, K.H.; Dabkowska, I.; Storoniak, P.; Rak, J.; Gutowski, M. AT base pair anions versus (9-methyl-a)(1-methyl-t) base pair anions. *J. Am. Chem. Soc.* **2005**, 127, 6443–6450.
49. Haranczyk, M.; Gutowski, M.; Li, X.; Bowen, Jr., , K.H. Bound anionic states of adenine. *Proc.Nat. Acad.Sci.* **2007**, 104, 4804–4807.
50. Mulliken, R.S. Iodine revisited. *J. Chem. Phys.* **1971**, 55, 288–309.